

Spectral atlas of dwarf novae in outburst

L. Morales-Rueda, T. R. Marsh

*Department of Physics and Astronomy, Southampton University, Southampton SO17 1BJ, UK
(lmr@astro.soton.ac.uk, trm@astro.soton.ac.uk)*

Accepted ... Received ...; in original form ...

ABSTRACT

Up to now, only a very small number of dwarf novae have been studied during their outburst state (~ 30 per cent in the Northern hemisphere). In this paper we present the first comprehensive atlas of outburst spectra of dwarf novae. We study possible correlations between the emission and absorption lines seen in the spectra and some fundamental parameters of the binaries. We find that out of the 48 spectra presented, 12 systems apart from IP Peg show strong HeII in emission: SS Aur, HL CMa, TU Crt, EM Cyg, SS Cyg, EX Dra, U Gem, HX Peg, GK Per, KT Per, V893 Sco, IY UMa, and 7 others less prominently: FO And, V542 Cyg, BI Ori, TY Psc, VZ Pyx, ER UMa, and SS UMi. We conclude that these systems are good targets for finding spiral structure in their accretion discs during outburst if models of Smak (2001) and Ogilvie (2001) are correct. This is confirmed by the fact that hints of spiral asymmetries have already been found in the discs of SS Cyg, EX Dra and U Gem.

Key words:

accretion, accretion discs – binaries: spectroscopic – line: profiles – stars: mass-loss – stars: novae, cataclysmic variables.

1 INTRODUCTION

Dwarf novae are a type of cataclysmic variable that undergo outbursts during which they increase in brightness by 2–8 mags. The outburst recurrence time varies widely from system to system and can be as short as a few days (ER UMa systems) and as long as tens of years (WZ Sge systems). The most likely mechanism for dwarf nova outbursts is a thermal instability within an accretion disc (Osaki 1974). There are still many unknowns in the disc instability theory. For example, although we know that the viscosity in the disc plays a fundamental role in driving the outburst, we do not know what its origin is. In 1986 Sawada, Matsuda & Hachisu suggested that the disc viscosity could be due to shocks in the disc tidally excited by the donor star. In 1991, Balbus & Hawley discovered a strong magneto-hydrodynamical instability of accretion discs which can indeed produce considerable effective viscosity. But it is not yet certain which, if either, of these is dominant.

There are several extensive studies on dwarf novae in the literature (Warner 1995 and references therein) but they concentrate mainly on their quiescent states. Only ~ 30 per cent of known Northern hemisphere dwarf novae have published outburst spectra and the number for Southern hemisphere systems is even smaller. The main aim of this paper is to fill this gap by presenting spectra of 48 dwarf novae

during their outburst state. We carry out comparisons between the spectra of the different dwarf novae and search for possible correlations between the features seen in the spectra and fundamental parameters of the systems such as their inclination, the mass of their components, their orbital periods and the outburst phases at which they were observed. Comparisons between the spectra are possible because the data were taken with comparable setups during a long term programme using service time.

Another reason for compiling this atlas is to look for spectra similar to that of IP Peg, U Gem and WZ Sge, systems that have been confirmed to show spiral structure in their discs during outburst. By confirmed we mean that spiral structure has been detected in more than one set of data, either taken during a different outburst or during the same outburst at a different time (IP Peg: Steeghs et al. 1997, Harlaftis et al. 1999, Morales-Rueda, Marsh & Billington 2000; U Gem: Groot 2001, Steeghs private communication; WZ Sge: Kuulkers et al. 2001, Baba, Sadakane & Norimoto 2001). The principal feature of their spectra, compared with those of other dwarf novae, is that they show strong lines in emission instead of absorption. Of the ~ 30 per cent of dwarf novae with outburst spectra published, only half of these show any emission, and even then it is often in the form of emission lines buried in absorption troughs. There could easily be systems with strong emission lines in outburst that

arXiv:astro-ph/0201367v1 22 Jan 2002

have yet to be identified. Of most interest is the presence of He II $\lambda 4686 \text{ \AA}$ in emission as this line is very important from the irradiation point of view. If these asymmetric structures seen in the discs of IP Peg, U Gem and WZ Sge are the result of tidally thickened sectors of the disc being irradiated by the white dwarf, boundary layer and/or inner disc during the outburst (as suggested by Smak 2001 and Ogilvie 2001) we expect them to be seen most clearly in He II $\lambda 4686 \text{ \AA}$.

2 OBSERVATIONS

The data presented in this paper were taken by different support astronomers during service time. All the spectra but two were obtained with the Intermediate Dispersion Spectrograph (IDS) mounted on the 2.5 m Isaac Newton telescope (INT) on La Palma. The spectra of IR Gem and IY UMa were taken with the blue arm of ISIS on the 4 m William Herschel telescope (WHT). Two different IDS setups were used for the observations. The first setup consisted of the 235 mm camera with the R1200B grating. The second setup used the 500 mm camera and the R632V grating. The observations were taken with one of the two CCDs available with the IDS, either the thinned EEV10 (2Kx4K) or the Tek (1Kx1K). Both setups produced almost the same wavelength dispersion (35 and 31 \AA mm^{-1} respectively). In both cases we covered H γ and He II $\lambda 4686 \text{ \AA}$ and a few He I lines. The two spectra taken with the WHT used the blue arm of ISIS with the R1200B grating and a EEV CCD covering the same wavelength region as the INT spectra with a wavelength dispersion of 33 \AA mm^{-1} . Exposure times were generally 600 s. Table 1 gives a list of the dwarf novae observed.

The images were debiased and flat-fielded using bias and tungsten lamp exposures respectively. The optimal extraction algorithm of Horne (1986) was used to extract the spectra. The data were wavelength calibrated using a CuAr arc lamp. The arcs were extracted using the profile determined for their corresponding stellar image to avoid possible systematic errors due to tilted spectra. We observed one flux standard with each of the setups: BD+28 $^{\circ}$ 4211 (Oke 1990) with the first setup on 2000 August 15, BD+33 $^{\circ}$ 2642 (Oke 1990) with the second setup on 2000 April 10, and HD19445 (Oke & Gunn 1983) with the WHT on 2000 January 18. These were used to correct the data from instrumental response and extinction.

3 RESULTS

Figs. 1 to 8 present the spectra of 48 dwarf novae during their outburst state. Above the spectra there is another panel showing the VSNET (Variable Star Network), VSOLJ (Variable Star Observers League in Japan) or AAVSO (American Association of Variable Star Observers) lightcurve with an arrow pointing at the time when our spectra were taken. For those systems where there are very few data points in the light curves we have also plotted a horizontal dashed line indicating the magnitude of the quiescent state as given by Downes, Webbink & Shara (1997). Of all the dwarf novae presented, only a few were observed on the same night as the standards used for their flux calibration:

FO Aql, LX And, IR Gem, IP Peg, GK Per, V893 Sco, NY Ser, IY UMa and SS UMi. For the other 39 systems we used the standard taken with the same setup as the targets to calibrate their fluxes. In these cases the slope of the continuum should be taken with caution. Most of the spectra show a blue continuum characteristic of cataclysmic variables. An exception to this is SS Aur that seems to show a red excess in the continuum. We do not believe this to be real but the result of incorrect flux calibration. We have not been able to track down the problem in this case. After flux calibration, we divided each spectrum by a constant obtained by averaging the values of the continuum in regions free of lines. We plot all the spectra from zero to show the relative line strengths.

Table 3 gives the measured equivalent width (EW) and full width at half maximum (FWHM) of the lines present in the spectra as well as the inclination and masses of the compact object and the donor star when known, as taken from Ritter & Kolb (1998) unless otherwise indicated. To measure EWs we considered the absorption lines to extend from -3500 km s^{-1} to 3500 km s^{-1} for the Balmer lines and from -3000 km s^{-1} to 3000 km s^{-1} for the He I lines. For emission lines with no sign of absorption we considered the line to comprise from -1000 km s^{-1} to 1000 km s^{-1} of the rest wavelength. In the case of He II $\lambda 4686 \text{ \AA}$ we tried to avoid contamination by the nearby Bowen blend and He I $\lambda 4713 \text{ \AA}$ by choosing the line limits by eye in each case. In the particular case of IY UMa only the EW of H β is reliable as H γ and He II $\lambda 4686 \text{ \AA}$ are heavily contaminated by nearby lines. FWHMs were measured by fitting a Gaussian function to the emission or absorption line. The FWHM, the offset from the rest wavelength, and the peak of the Gaussian were free parameters of the fit. In the case of absorption lines with emission cores, the FWHM of the absorption component were measured by masking the central emission. In those cases, two values for FWHM are given, one for the absorption line and another for the central emission. In the case of emission lines with absorption cores, the absorption was also masked before the Gaussian fit was attempted but only the emission FWHM is given.

For comparison we have also included the spectra of GK Per during its 1996 outburst (Morales-Rueda, Still & Roche 1999) and that of IP Peg, during its August 1994 outburst (Morales-Rueda et al. 2000). The spectrum of IP Peg is very different from that of the rest of the dwarf novae, the most striking difference being the strong He II $\lambda 4686 \text{ \AA}$ line in emission.

3.1 Notes on particular objects

SS Aur. As noted above, the red continuum seen in the spectra of this system is probably the result of poor flux calibration.

SS Cyg. We took two spectra of this dwarf nova during the same outburst, one near maximum, the other in the descent to quiescence. The spectra at these two times show some major differences. At maximum the continuum increases significantly. As a result of the disc becoming optically thick, we see absorption lines with an emission core. The strength of the He II $\lambda 4686 \text{ \AA}$ line is significantly larger relative to the strength of the Balmer and He I lines com-

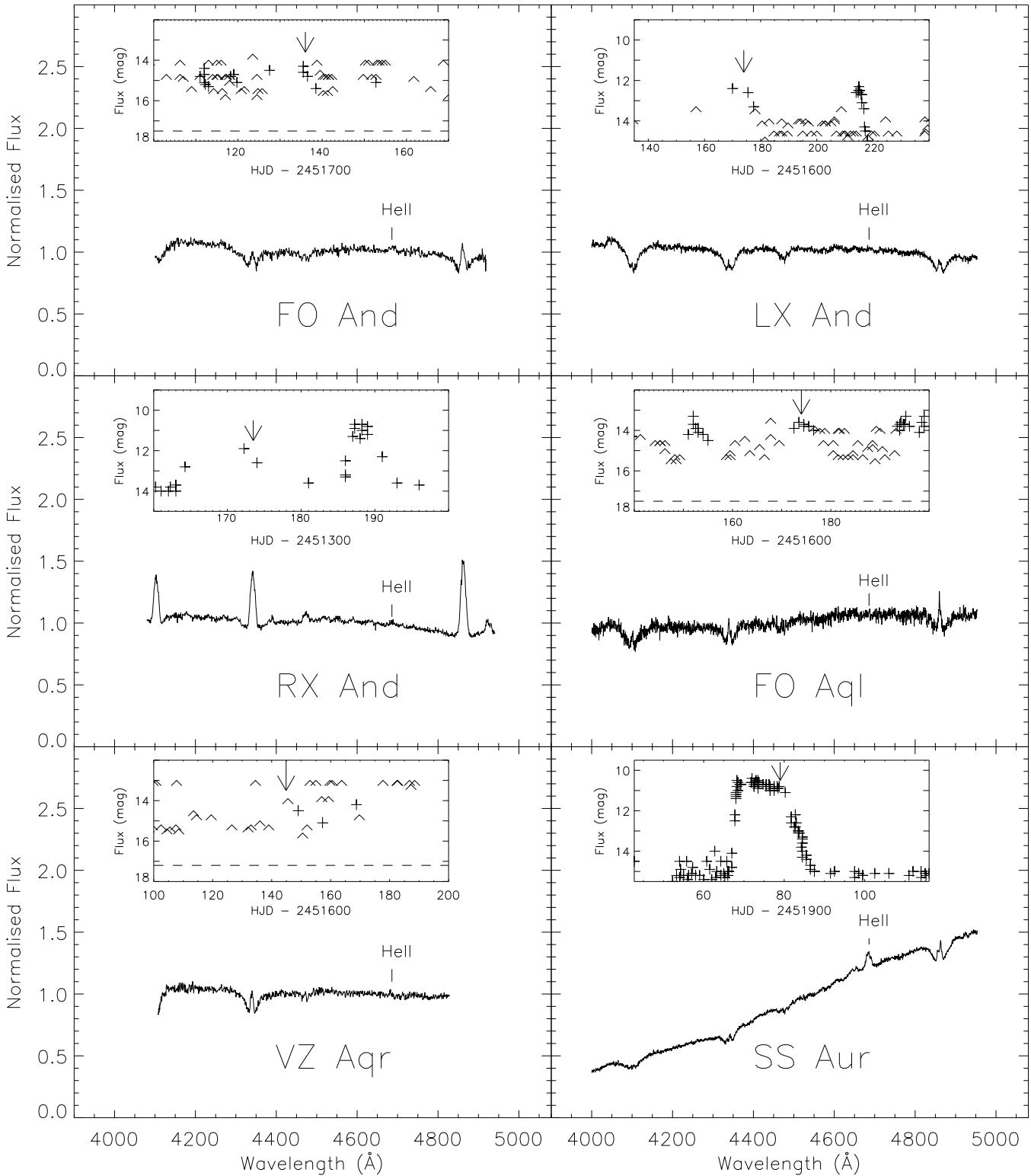


Figure 1. Outburst spectra of 6 dwarf novae. Each panel contains the spectrum of the object and another panel with its lightcurve. An arrow indicates the time when the spectrum was taken. A horizontal dashed line indicates the magnitude of the quiescent level as given by Downes et al. (1997). The normalised flux is plotted from zero to show the relative line strengths with respect to the continuum. See text for more details.

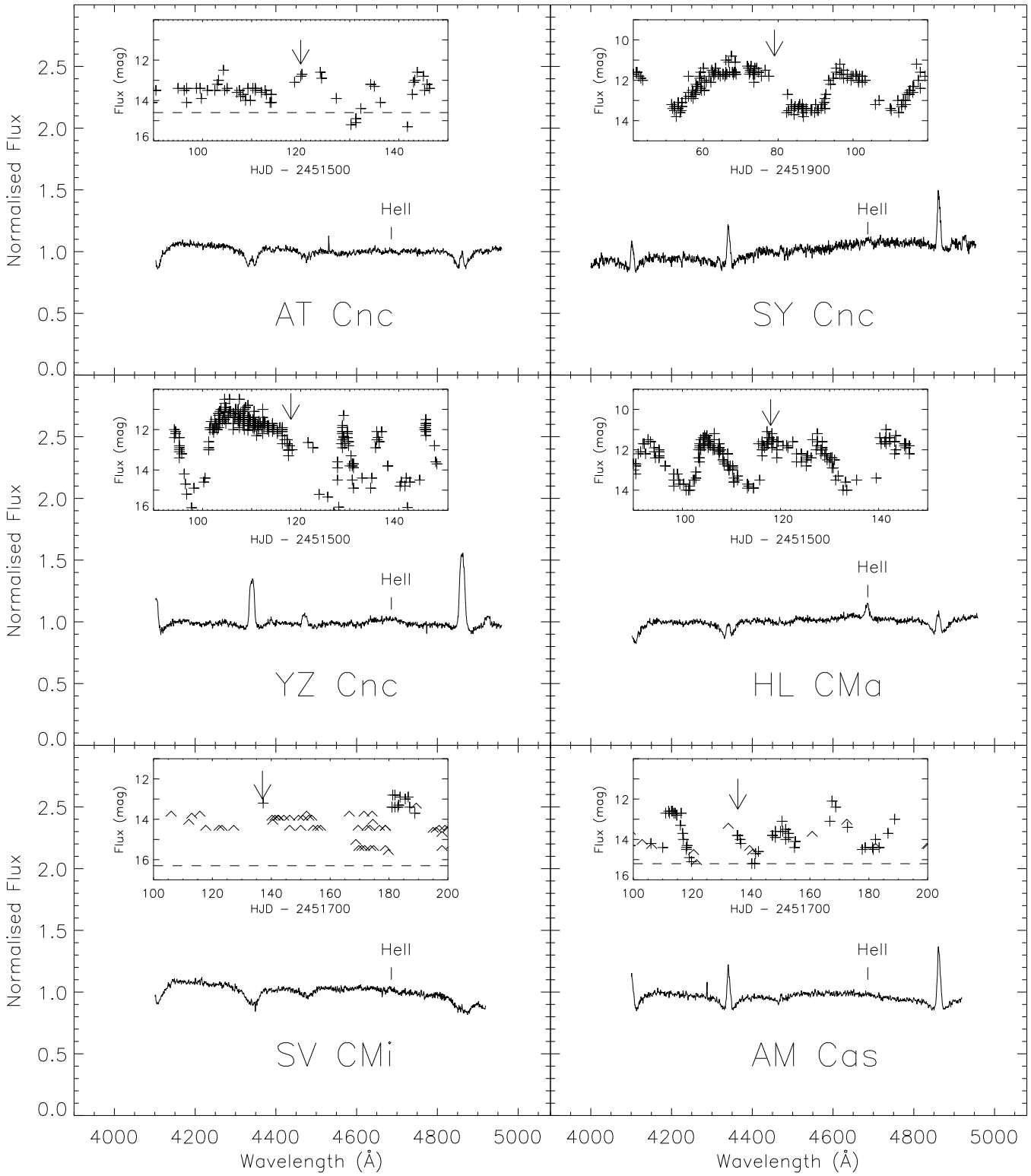


Figure 2. Same as in Fig. 1.

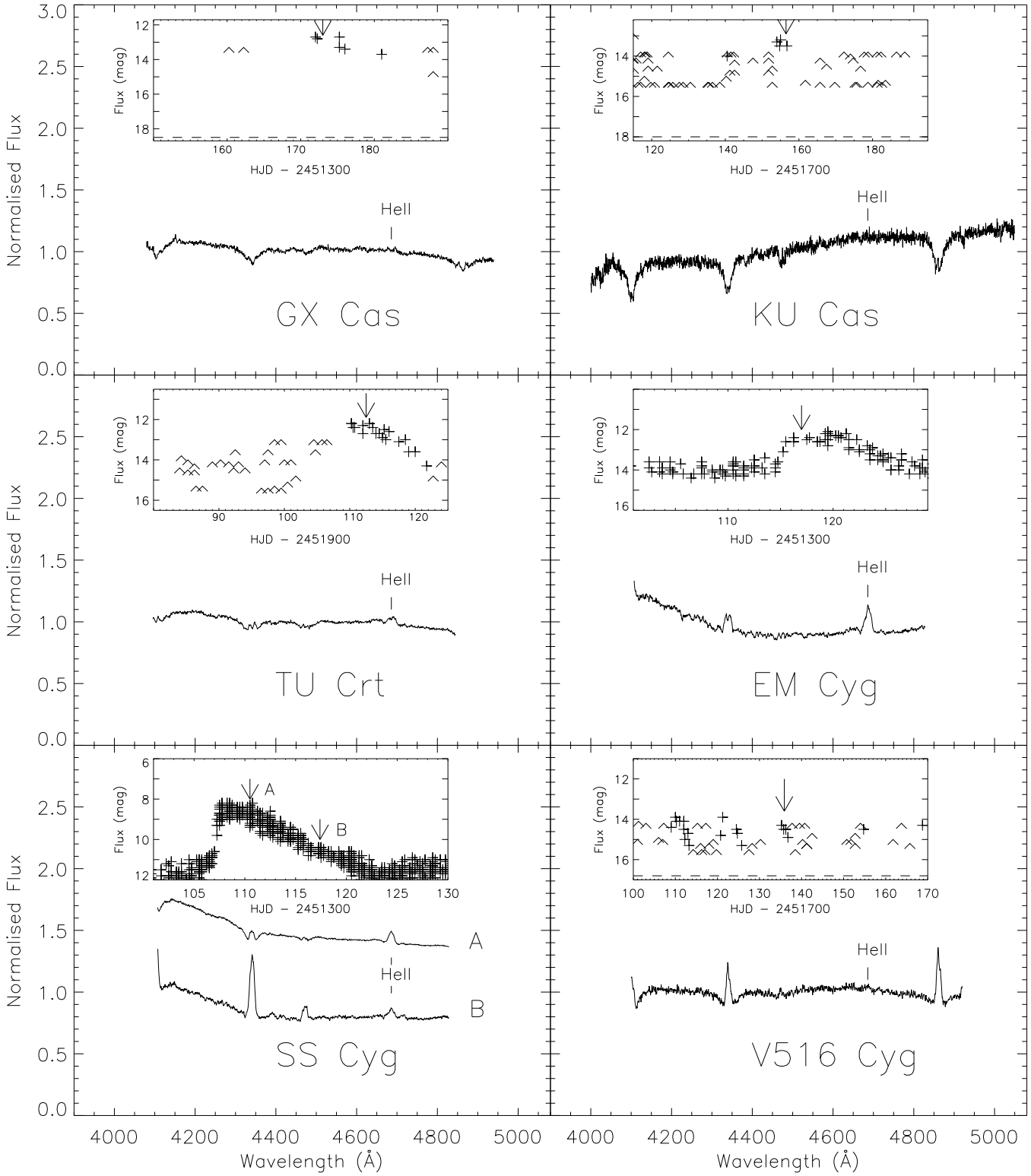


Figure 3. Same as in Fig. 1.

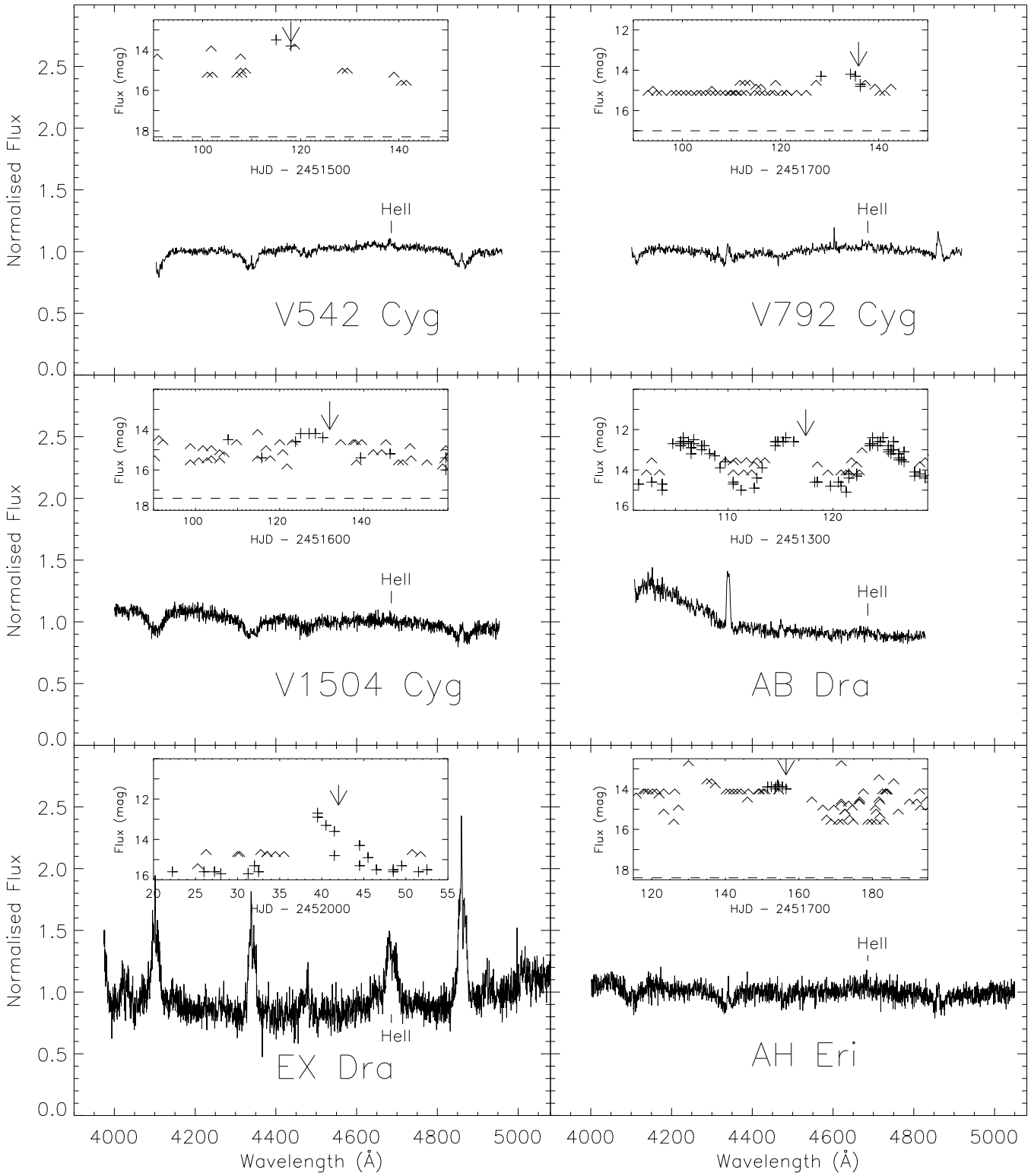


Figure 4. Same as in Fig. 1.

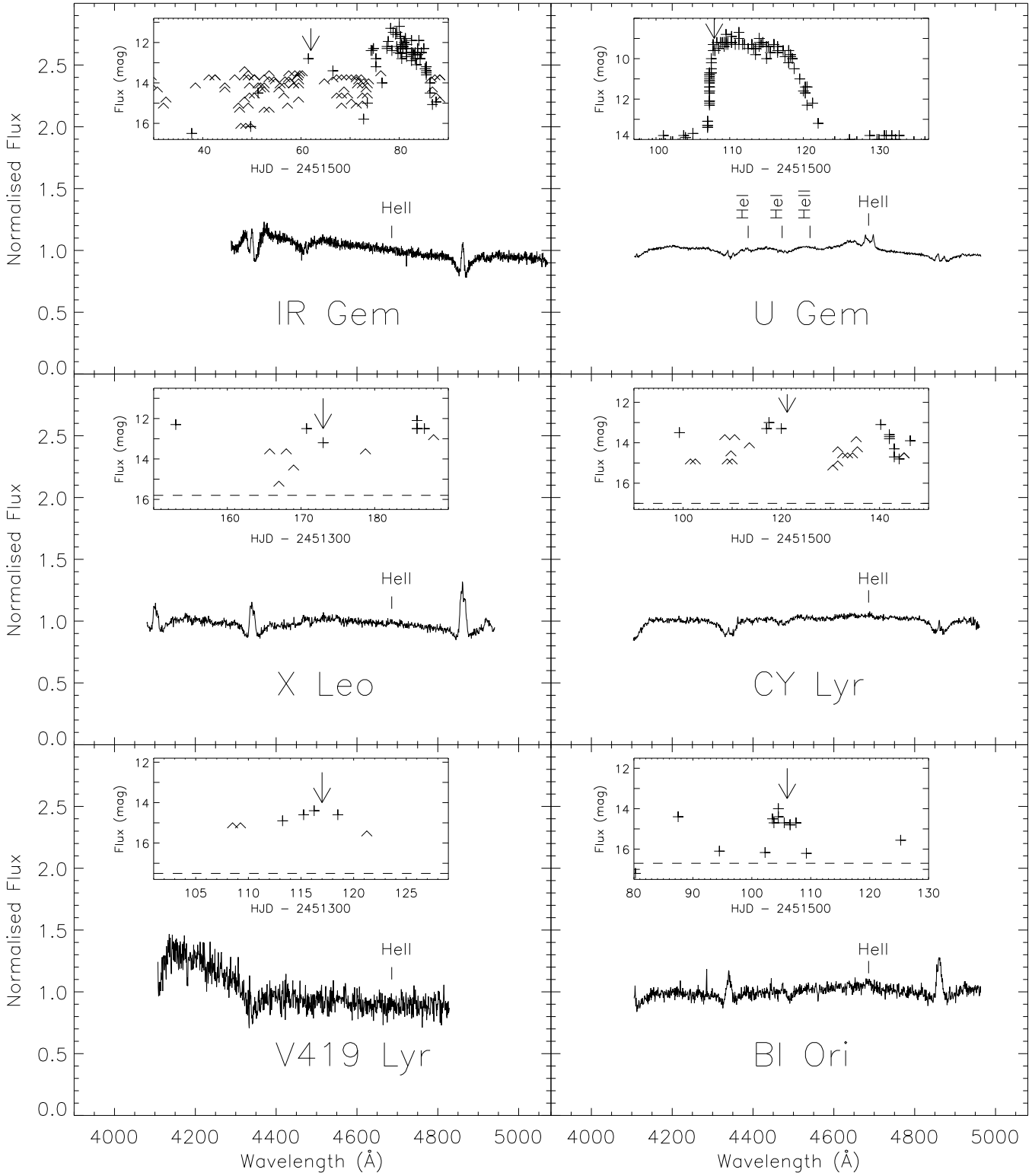


Figure 5. Same as in Fig. 1.

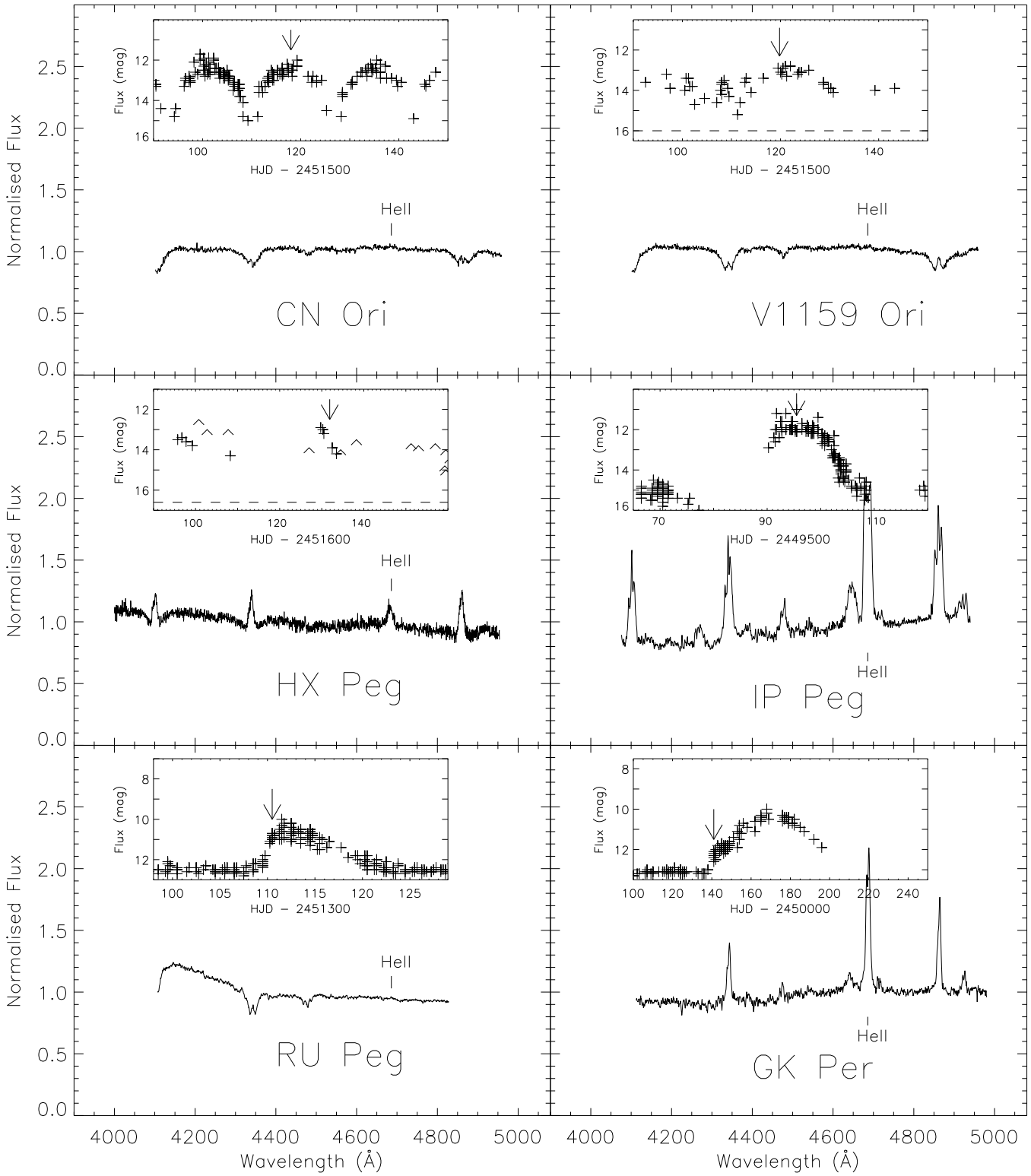


Figure 6. Same as in Fig. 1.

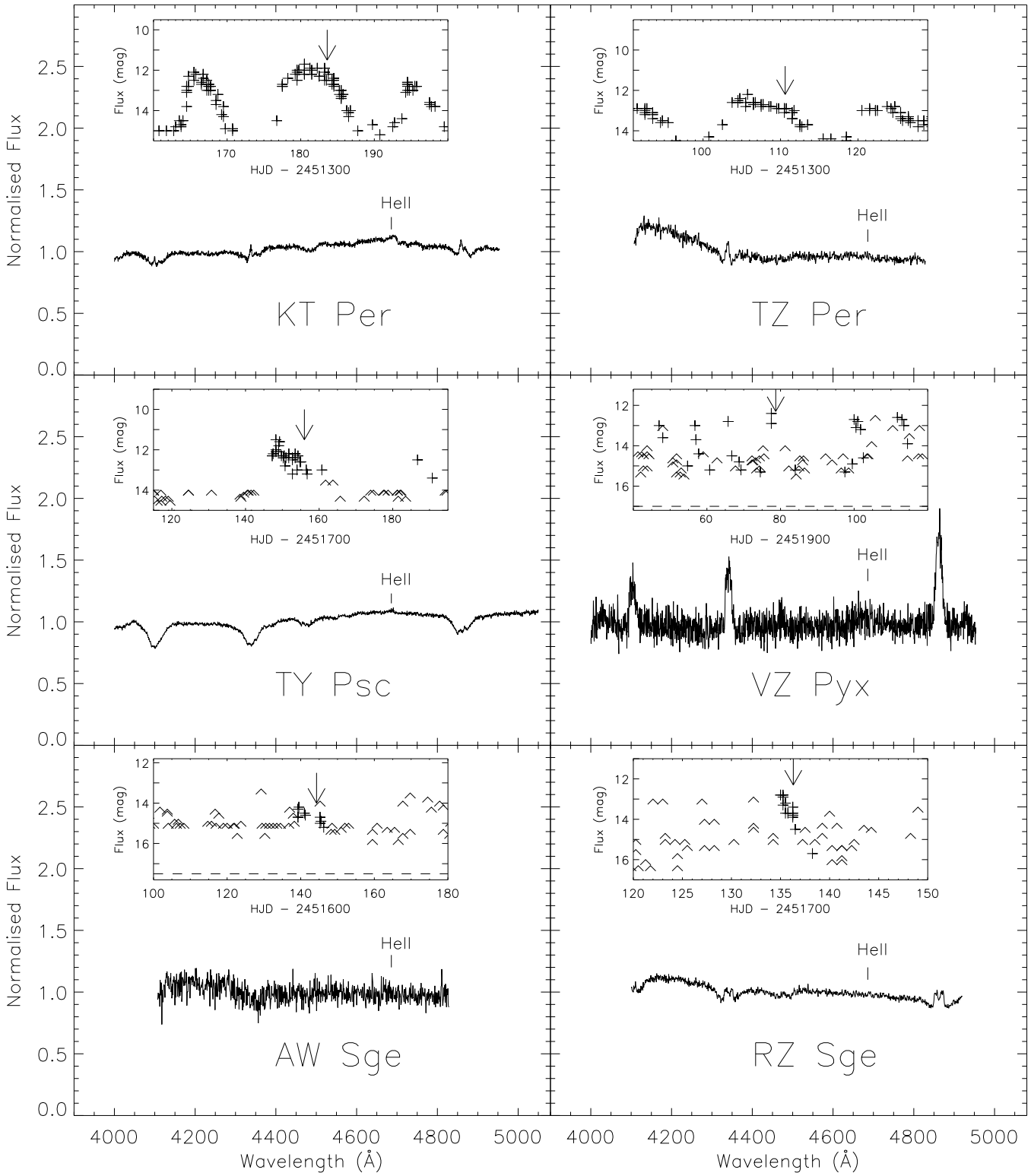


Figure 7. Same as in Fig. 1.

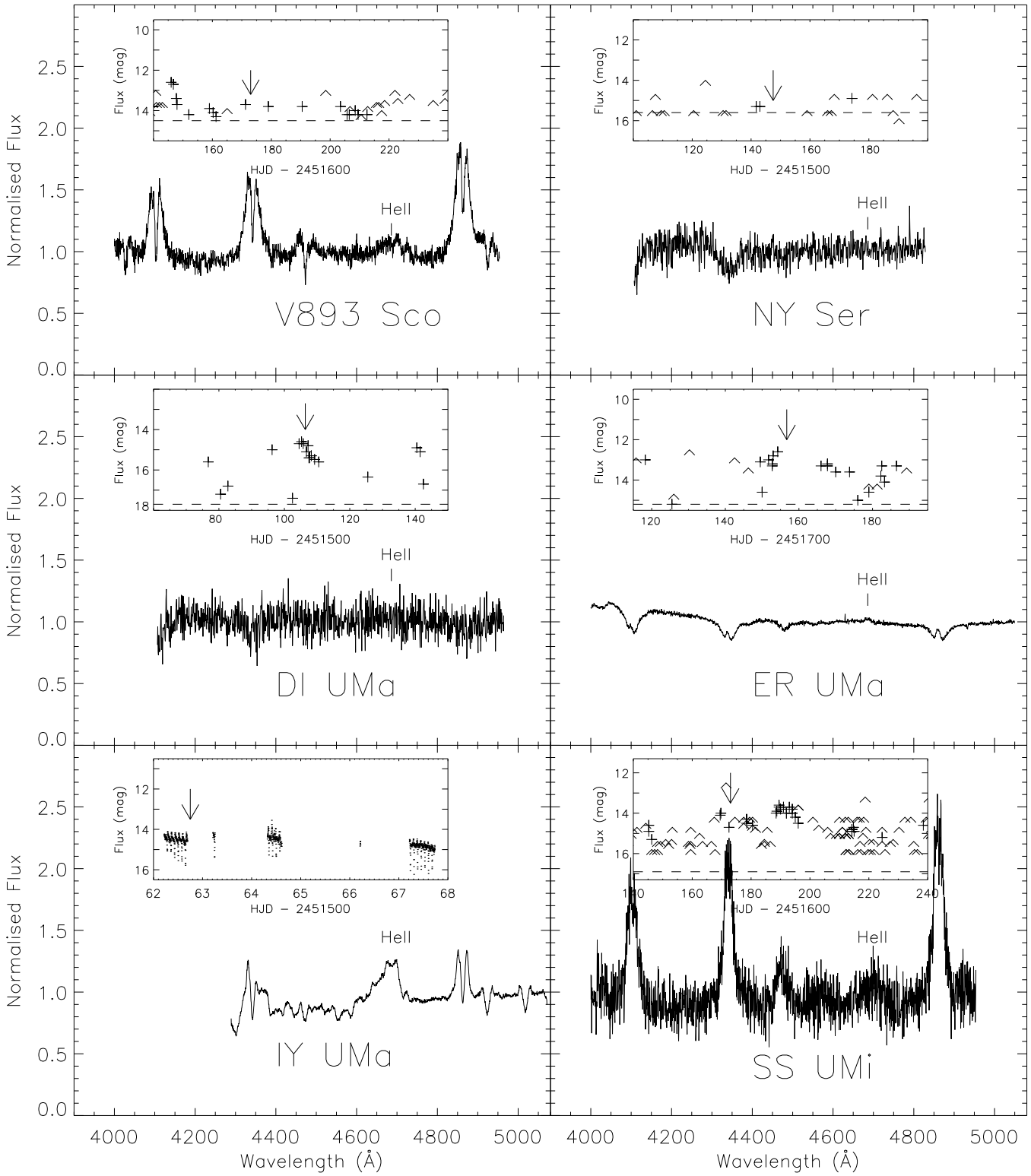


Figure 8. Same as in Fig. 1.

Table 1. List of the dwarf novae (DNe) in outburst observed during this program. A note is added when the dwarf nova is of the SU UMa or Z Cam type (shows superoutbursts or standstills as well as normal outbursts). The date when the system was observed is given as well as its orbital period, P_{orb} , when known (Ritter & Kolb 1998, (a) Thorstensen 1997, (b) Uemura et al. 2000). All DNe were observed using the INT except IR Gem and IY UMa which were observed with the WHT.

Target	DNe type	Date observed	P_{orb} (d)	Target	DNe type	Date observed	P_{orb} (d)
FO And	suuma	2000/10/17	0.0716	IR Gem	suuma	2000/01/18	0.0684
LX And		2000/08/15		U Gem		2000/03/02	0.1769
RX And	zcam	2000/10/21	0.2099	X Leo		1999/10/21	0.1644
FO Aql		2000/08/15		CY Lyr		2000/03/14	0.1591
VZ Aqr		1999/07/16		V419 Lyr	zcam	1999/08/26	
SS Aur		2001/03/07	0.1828	BI Ori		2000/03/02	
AT Cnc	zcam	2000/03/14	0.2387	CN Ori	zcam	2000/03/14	0.1632
SY Cnc	zcam	2001/03/07	0.3800	V1159 Ori	suuma	2000/03/14	0.0622
YZ Cnc	suuma	2000/03/14	0.0868	HX Peg		2000/07/03	0.2008
HL CMa	zcam	2000/03/14	0.2145	IP Peg		1994/08/30	0.1582
SV CMi	zcam	2000/10/17	0.1560	RU Peg		1999/08/19	0.3746
AM Cas	zcam	2000/10/17	0.1650	GK Per		1996/02/28	1.9968
GX Cas	suuma	1999/10/21	0.0890	KT Per	zcam	1999/10/31	0.1627
KU Cas		2000/11/6		TZ Per	zcam	1999/08/19	0.2605
TU Crt	suuma	2001/04/11	0.0844	TY Psc	suuma	2000/11/6	0.0683
EM Cyg	zcam	1999/08/26	0.2909	VZ Pyx	suuma	2001/03/07	0.0740
SS Cyg		1999/08/19,26	0.2751	AW Sge		2000/07/16	
V516 Cyg		2000/10/17		RZ Sge	suuma	2000/10/17	0.0686
V542 Cyg		2000/03/14		V893 Sco		2000/08/15	0.0761
V792 Cyg		2000/10/17		NY Ser	suuma	2000/04/10	0.1007
V1504 Cyg	zcam	2000/07/03	0.0695	DI UMa		2000/03/02	0.0548
AB Dra	zcam	1999/08/26	0.1520	ER UMa	suuma	2000/11/6	0.0637
EX Dra		2001/05/09	0.2099	IY UMa	suuma	2000/01/18	0.0738 ^b
AH Eri		2000/11/6	0.2391 ^a	SS UMi	suuma	2000/08/15	0.0678

pared to the quiescent state. In contrast, the spectrum taken near quiescence shows a lower continuum with Balmer and He emission lines. SS Cyg is one of the systems claimed to have spiral asymmetries during outburst (Steehgs et al. 1996).

U Gem. The spectrum shows Balmer absorption lines with faint emission cores. He II $\lambda 4686 \text{ \AA}$ appears strong in the spectrum and double peaked presumably due to the high inclination of the system. There is also some emission in the Bowen blend. In a recent study of U Gem during outburst Groot (2001) finds spiral structure in the accretion disc. Spectra taken on 2001 April 30, and May 4, 5, 9 and 10 when U Gem was in outburst (first three nights) and decaying to quiescence (last two nights) show the presence of spiral structure in He II $\lambda 4686 \text{ \AA}$ and less clearly in H β while the system was in outburst. The He II $\lambda 4686 \text{ \AA}$ emission line disappears almost completely from the spectrum on May 9 and 10, when the system was half way down to its quiescent state (Steehgs, private communication). This indicates that the origin of He II $\lambda 4686 \text{ \AA}$ is either irradiation caused by a thickening of the accretion disc during outburst, as suggested by Ogilvie (2001), or the spiral asymmetries themselves.

Other features worth mentioning about the spectrum of U Gem are the bumpy structures seen to the blue of He II $\lambda 4686 \text{ \AA}$. These are seen in other spectra of this sample, i.e. KT Per, TY Psc, V516 Cyg. These features are real and correspond to multiple He I and Fe II lines. Some of them have been marked in the spectrum of U Gem for clarity.

AW Sge, NY Ser, DI UMa. These spectra are particularly noisy as these dwarf novae are still quite faint during outburst and our standard exposure time did not achieve the intended signal to noise. The signal-to-noise ratio of these spectra does not allow us to conclude whether He II $\lambda 4686 \text{ \AA}$ is present in emission or not but they clearly show Balmer lines in absorption, perhaps with central emission. They probably resemble the spectra of RU Peg or V1159 Ori more than that of IP Peg.

IY UMa. This spectrum shows strong Balmer and He I lines in emission with absorption cores (the opposite to what we have seen up to now). There is strong emission in He II $\lambda 4686 \text{ \AA}$ and the Bowen blend. Although from the light curve we can see that our spectrum does not coincide with amateur observations, we are certain that IY UMa was in outburst when we observed it as its quiescent level is magnitude ~ 17 . The rapid variations seen in the light curve are due to eclipses.

3.2 He II $\lambda 4686 \text{ \AA}$ in emission

Out of the sample of CVs observed we find, apart from IP Peg, 12 dwarf novae that show He II $\lambda 4686 \text{ \AA}$ in emission: SS Aur, HL CMa, TU Crt, EM Cyg, SS Cyg, EX Dra, U Gem, HX Peg, GK Per, KT Per, V893 Sco, IY UMa, and possibly 7 other systems where He II $\lambda 4686 \text{ \AA}$ is present but very faint: FO And, V542 Cyg, BI Ori, TY Psc, VZ Pyx, ER UMa, and SS UMi.

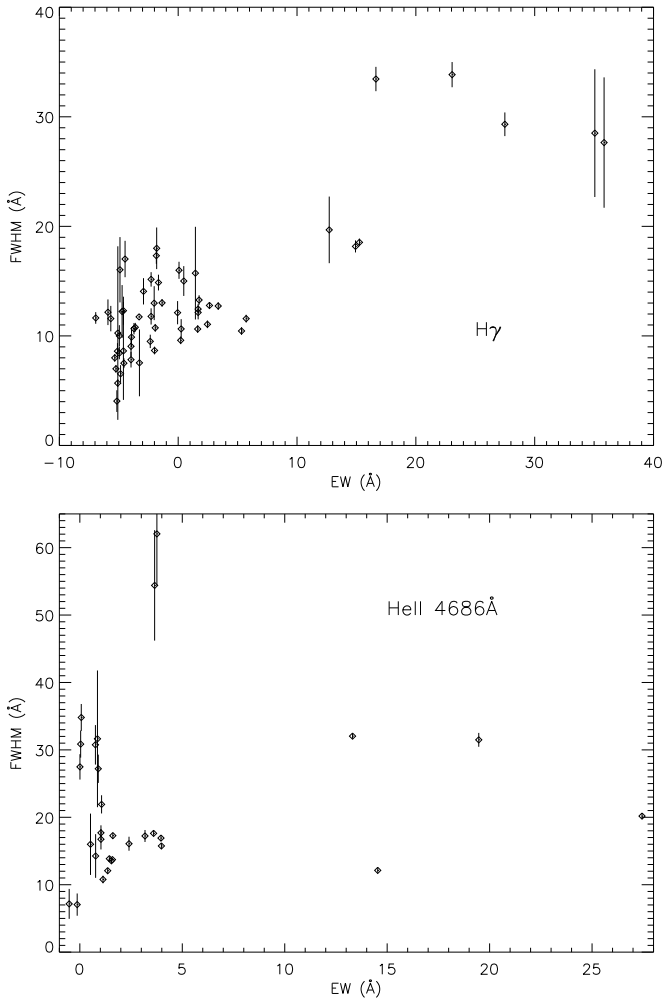


Figure 9. FWHM versus EW for $H\gamma$ (top panel) and $\text{He II } \lambda 4686 \text{ \AA}$ (bottom panel.)

4 DISCUSSION

In this section we look for correlations between the quantities we can measure in our spectra (i.e. EW, FWHM, outburst phase) and fundamental parameters of the dwarf nova, like their masses and orbital periods.

4.1 FWHM versus EW

For high inclination dwarf novae, the FWHM of the lines scales as $\sin i$ (where i is the inclination of the system). This is due to Doppler broadening of the lines. It is not clear that this is true for low inclination systems. At low inclinations other mechanisms may dominate over Doppler broadening, e.g. thermal broadening, intrinsic broadening. It is not possible to establish at what range of inclinations the FWHM of the lines is directly proportional to $\sin i$ because we are not capable of measuring $\sin i$ with any certainty for systems that are not eclipsing.

Keeping this in mind we search for correlations between the FWHM of the lines and their strength, as given by their

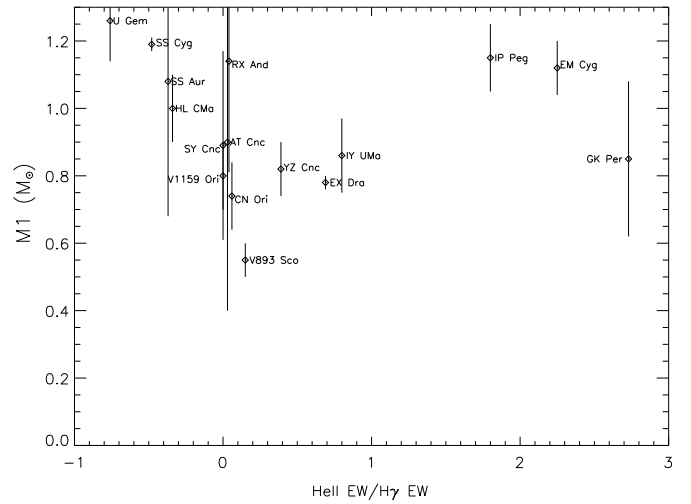


Figure 10. Mass of the white dwarf in the dwarf nova versus the ratio of equivalent widths of $\text{He II } \lambda 4686 \text{ \AA}$ and $H\gamma$.

EW. Fig. 9 shows the FWHM versus EW for $H\gamma$ (top panel) and $\text{He II } \lambda 4686 \text{ \AA}$ (bottom panel).

There is some indication of positive correlation of FWHM with EW. This apparent correlation would indicate that high inclination systems (those with higher FWHM) show stronger emission lines. It is worth mentioning that three of the systems where $\text{He II } \lambda 4686 \text{ \AA}$ is strong in emission during outburst and where spiral structure has been detected, i.e. IP Peg, EX Dra and U Gem, are edge-on systems and one expects radiative transfer effects to favour seeing emission in such cases.

4.2 Line emission versus the masses of the components of the system

Another property to be explored is the $\text{He II}/\text{Balmer}$ ratio which one might expect to depend upon white dwarf mass on the basis that accretion onto higher mass white dwarfs will produce more photons capable of ionising He II . In Fig. 10 we have plotted those two quantities for those systems where the mass of the white dwarf has been measured. There is no correlation apparent. In most cases the measurements of the masses of the compact objects have been performed by measuring the white dwarf radial velocity semi-amplitude and combining it with the radial velocity semi-amplitude of the companion star. Assuming a mass for the donor star depending on its spectral type, a value for the mass of the compact object is obtained. It is worth mentioning that this method is known to produce very uncertain results and that the uncertainties in the mass determinations could completely mask any such a relationship if it existed.

When we explore the correlation between the EW of the $\text{He II } \lambda 4686 \text{ \AA}$ line versus the mass of the compact object, the mass of the donor star, and the mass ratio of the system we reach the same conclusion: there is no correlation between the masses of the components of the binaries and the $\text{He II } \lambda 4686 \text{ \AA}$ EW. It is worth emphasising again that the values for the white dwarf masses are very uncertain. Also we should not forget that the EWs of the lines can

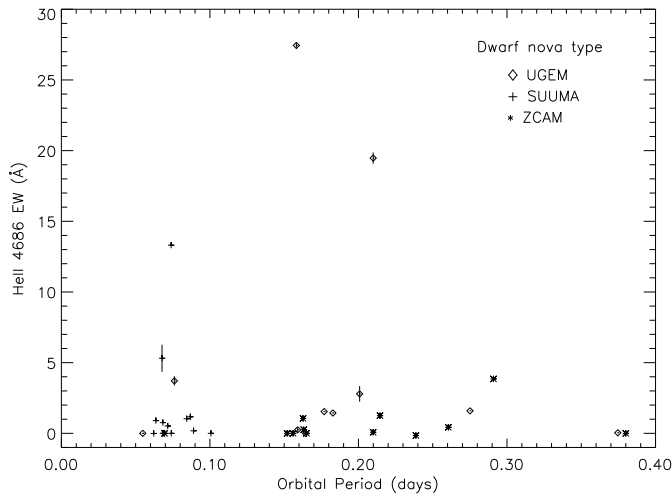


Figure 11. He II $\lambda 4686$ Å equivalent width versus the orbital period of the dwarf nova. Different symbols are used for each dwarf nova type.

change significantly for one system during the outburst, e.g. the He II $\lambda 4686$ Å EW of U Gem during its April/May 2001 outburst changes from -1 to 4 Å throughout the outburst (Steeghs private communication). The EW values plotted here are measured at a particular time during outburst that is not the same for all the systems plotted which again may mask any correlations.

4.3 Line emission versus orbital period

In Fig. 11 we present the EW of the He II $\lambda 4686$ Å line measured from each dwarf nova spectrum presented in this paper versus its orbital period (Ritter & Kolb 1998). As there is a correlation between the dwarf nova type and its orbital period, we have used different symbols for U Gem, SU UMA and Z Cam systems. It is clear that there is no correlation between the orbital period of the CV and the strength of the He II $\lambda 4686$ Å emission. The orbital periods of 9 of the dwarf novae presented in this study are unknown and therefore have not been included in this plot.

4.4 EW and FWHM versus outburst phase

We already mentioned in section 4.2 that the EW of one particular line might change considerably throughout the outburst. By introducing the concept of outburst phase, ϕ_{out} , (time since the start of the outburst divided by the length of the outburst) we can use our sample of dwarf novae to study whether there is any relationship between the EW and FWHM of the lines and the outburst phase at which they were observed. The outburst phases for the dwarf novae observed are given in Table 2. The top panel of Fig. 12 presents the FWHM and EW measured for H γ and He II $\lambda 4686$ Å. Two values for the FWHM of H γ are presented, one was measured when the line was in absorption and the other when the line was in emission or when the absorption line showed an emission core. The bottom panel of Fig. 12 shows

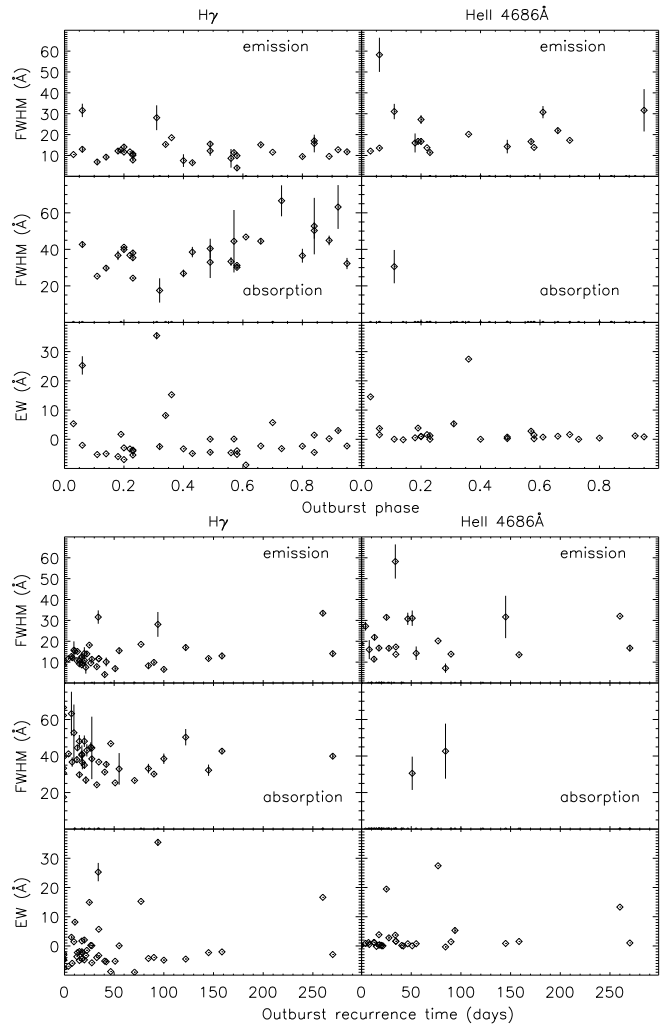


Figure 12. FWHM and EW for H γ and He II $\lambda 4686$ Å versus the outburst phase at which the dwarf novae were observed (top panels) and versus the average time between outbursts (bottom panels).

also the FWHM and EW for both lines but this time versus the average times between outbursts. We calculated these by using VSNET lightcurves that span over years. One of the dwarf novae, GK Per, has not been included in this bottom figure because its outburst recurrence time is ~ 1095 days (3 years) and expanding the scale that much would not allow us to see the other points.

It is clear from the plots that there is not any clear correlation between the FWHM and EW of the lines and the outburst phase or the average time between outbursts.

5 CONCLUSIONS

We present the first comprehensive sample of dwarf nova spectra during outburst. We study the possible correlations between the lines present in the spectra and fundamental parameters of the systems. We find that there is no correlation between the strength of the lines and the masses of the components of the system or the periods of the binaries.

Table 2. List of the dwarf novae and the outburst phase at which they were observed. The average outburst recurrence time (RT) in days as calculated by using VSNET data is also given.

Target	RT	ϕ_{out}	Target	RT	ϕ_{out}
FO And	8	0.18	IR Gem	33	0.23
LX And	41	0.58	U Gem	159	0.06
RX And	20		X Leo	23	
FO Aql	22	0.40	CY Lyr	20	
VZ Aqr	85		V419 Lyr	350	
SS Aur	90	0.58	BI Ori	55	0.49
AT Cnc	15	0.14	CN Ori	18	0.49
SY Cnc	27	0.89	V1159 Ori	42	0.23
YZ Cnc	7	0.92	HX Peg	28	0.57
HL CMa	13	0.23	IP Peg	77	0.36
SV CMi	28		RU Peg	51	0.11
AM Cas	18		GK Per	1095	0.03
GX Cas			KT Per	13	0.66
KU Cas	71		TZ Per	18	0.80
TU Crt	270	0.20	TY Psc	47	0.61
EM Cyg	18	0.19	VZ Pyx	11	0.34
SS Cyg	35	0.22,0.70	AW Sge		0.73
V516 Cyg	15		RZ Sge	122	0.84
V542 Cyg			V893 Sco	34	0.06
V792 Cyg	145	0.95	NY Ser		
V1504 Cyg		0.56	DI UMa		0.32
AB Dra	10	0.84	ER UMa	4	0.20
EX Dra	25		IY UMa	260	
AH Eri	100	0.43	SS UMi	94	0.31

There seems to be some correlation between the strength of the lines and the inclination of the system as represented by the FWHM of the lines. We do not find any correlation between the FWHM or the EW of the lines and either the time of the outburst at which the dwarf novae were observed or the outburst recurrence time measured for each system.

Of the 48 dwarf novae outburst spectra presented we find that 20 systems, 13 of them very clearly, and the other 7 possibly, show He II $\lambda 4686 \text{ \AA}$ in emission. If models presented by Smak (2001) and Ogilvie (2001) are correct, these are good candidates to show spiral structure in their accretion discs during outburst. These results are even more encouraging because four of these candidates: SS Cyg, EX Dra, U Gem and IP Peg, have been seen to show hints of spiral structure in their discs already (Steeghs et al. 1996; Joergens, Spruit & Rutten 2000, Steeghs, Harlaftis & Horne 1997, Groot 2001). Based on recent outburst spectra of U Gem (Steeghs, private communication) we suggest that in fact the He II $\lambda 4686 \text{ \AA}$ emission is either the result of irradiation or produced by the spiral structures themselves. If its origin is irradiation we expect the He II $\lambda 4686 \text{ \AA}$ intensity to change with disc thickness. If the origin of He II $\lambda 4686 \text{ \AA}$ is the structures themselves, we should see them in all dwarf novae that show He II $\lambda 4686 \text{ \AA}$ emission. Time resolved spectroscopy of the other candidates found in our sample will allow us to confirm or dismiss the presence of spiral asymmetries in their accretion discs.

Acknowledgements

LM-R was supported by a PPARC post-doctoral research grant. The Isaac Newton telescope is operated on the island

of La Palma by the Isaac Newton Group in the Spanish Observatorio del Roque de los Muchachos of the Instituto de Astrofísica de Canarias. The authors would like to thank the Variable Star Network, VSNET, and the Variable Star Observers League in Japan, VSOLJ, for making their data available as most of the light curves presented in this paper were produced using their observations. In this research, we have used, and acknowledge with thanks, data from the AAVSO International Database, based on observations submitted to the AAVSO by variable star observers worldwide. The reduction and analysis of the data was carried out on the Southampton node of the STARLINK network. We also wish to thank the referee and D. Steeghs for useful comments and L. González Hernández for computer support.

REFERENCES

- Baba H., Sadakane K., Norimoto Y., 2001, IAUC 7672
Balbus S., Hawley J., 1991, ApJ, 376, 214
Downes R. A., Webbink R. D., Shara M. M., 1997, PASP, 109, 345
Groot P., 2001, ApJL, 551, L89
Harlaftis E. T., Steeghs D., Horne K., Martín E., Magazzú A., 1999, MNRAS, 306, 348
Horne K., 1986, PASP, 98, 609
Joergens V., Spruit H. C., Rutten R. G. M., 2000, A&A, 356, L33
Kuulkers E., Knigge C., Steeghs D., Wheatley P., Long K. S., 2002, to appear in the ASP Conference Series, The Physics of Cataclysmic Variables and Related Objects, Eds B. T. Gänsicke, K. Beuermann, K. Reinsch (astro-ph/0110064)
Matsumoto K., Mennickent R. E., Kato T., 2000, A&A, 363, 1029
Morales-Rueda L., Marsh T. R., Billington I., 2000, MNRAS, 313, 454
Morales-Rueda L., Still M. D., Roche P., 1999, MNRAS, 306, 753
Morales-Rueda L., Still M. D., Roche P., Wood J. H., Lockley J. J., 2002, MNRAS, 329, 597
Nogami D., Masuda S., Kato T., Hirata R., 1999, PASJ, 51, 115
North R. C., Marsh T. R., Moran C. K., Kolb U., Smith R. C., Stehle R., 2000, MNRAS, 313, 383
Ogilvie G. I., 2002, MNRAS, in press (astro-ph/0111262)
Oke J. B., 1990, AJ, 99, 1621
Oke J. B., Gunn J. E., 1983, ApJ, 266, 713
Osaki Y., 1974, PASJ, 26, 429
Patterson J., Kemp J., Jensen L., Vanmunster T., Skillman D. R., Martin B., Fried R., Thorstensen J. R., 2000, PASP, 112, 1567
Ritter H., Kolb U., 1998, A&AS, 129, 83
Sawada E., Matsuda T., Hachisu I., 1986, MNRAS, 219, 75
Steeghs D., Harlaftis E. T., Horne K., 1997, MNRAS, 270, L28
Steeghs D., Horne K., Marsh T. R., Donati J. F., 1996, MNRAS, 281, 626
Szkody P., Linnell A., Honeycutt K., Robertson J., Silber A., Hoard D. W., Pastwick L., Desai V., Hubeny I., Cannizzo J., Liller W., Zissell R., Walker G., 1999, ApJ, 521, 362
Smak J. I., 2001, Acta Astron., 51, 295
Thorstensen J. R., 1997, PASP, 109, 1241
Uemura M., et al., 2000, PASJ, 52, L9
Warner B., 1995, Cambridge Astrophysics Series 28. Cataclysmic Variable Stars. Cambridge Univ. Press, Cambridge

Landscape table to go here

Table 3.

Table 3. Measurements for all the DNe observed. The values for the masses of the components of the dwarf novae (M_1 = mass of the white dwarf, M_2 = mass of the donor star) were taken from Ritter & Kolb (1998) unless otherwise indicated.(a) Nogami et al. (1999), (b) North et al. (2000), (c) Szkody et al. (1999), (d) Morales-Rueda et al. (2002), (e) Matsumoto, Mennickent & Kato (2000), (f) Patterson et al. (2000).

Target	i	EW (H β)	EW (H γ)	EW (HeII)	FWHM (H β)		FWHM (H γ)		FWHM (HeII)		$M_1(M_\odot)$	$M_2(M_\odot)$
					Emission	Absorption	Emission	Absorption	Emission	Absorption		
FO And	-	-2.94±0.24	-5.91±0.21	0.52±0.12	10.16±0.60	39.87±3.72	12.16±1.17	36.69±2.56	16.00±4.55	-	-	-
LX And	-	-4.83±0.08	-5.16±0.07	0.19±0.06	8.59±0.62	36.68±0.97	4.05±0.99	31.22±0.66	-	-	-	-
RX And	51±9	7.93±0.89	2.05±0.58	0.08±0.06	13.20±0.30	-	10.85±0.30	48.12±3.14	-	-	1.14±0.33	0.48±0.03
FO Aql	-	-3.53±0.17	-3.26±0.17	0.03±0.13	6.63±0.44	40.64±2.54	7.54±3.05	26.83±2.08	-	-	-	-
VZ Aqr	-	-	-4.27±0.42	-0.33±0.27	-	-	8.28±1.09	33.12±2.59	7.11±2.22	42.66±15.07	-	-
SS Aur	38±16	-3.46±0.04	-3.93±0.06	1.44±0.03	8.84±0.32	36.86±0.57	9.89±0.92	30.16±0.70	13.86±0.34	-	1.08±0.40	0.39±0.02
AT Cnc	17±5/36±12	-5.05±0.21	-4.95±0.09	-0.15±0.07	-	-	9.22±1.11	29.75±1.37	-	-	0.9±0.5 ^a	0.47±0.05
SY Cnc	26±6	1.53±0.10	0.21±0.17	-	8.74±0.14	48.85±4.59	9.60±0.18	44.88±2.62	-	-	0.89±0.28	1.10±0.05
YZ Cnc	38±3	6.26±0.58	3.00±0.52	1.17±0.13	-	-	12.76±0.29	63.19±12.00	-	-	0.82±0.08	0.17±0.08
HL CMa	45	-2.96±0.88	-3.67±0.09	1.25±0.16	-	-	10.73±0.52	38.03±1.72	11.43±0.92	-	1.0	0.45±0.1
SV CMi	-	-3.70±0.16	-5.76±0.14	-	-	33.32±2.13	-	38.46±1.12	-	-	-	-
AM Cas	-	1.90±0.15	-1.99±0.14	-	8.74±0.14	39.17±3.17	8.67±0.20	40.99±2.02	-	-	-	-
GX Cas	-	-3.2±0.491	-4.56±0.13	0.18±0.09	-	-	-	39.43±3.92	-	-	-	-
KU Cas	-	-8.76±0.18	-8.97±0.18	-	-	32.36±0.82	-	26.64±0.54	-	-	-	-
TU Crt	-	-	-2.92±0.06	1.03±0.04	-	-	14.07±1.20	39.92±1.36	16.74±1.51	-	-	-
EM Cyg	65±4	-	1.71±0.11	3.85±0.21	-	-	12.62±0.63	-	16.76±0.94	-	1.12±0.08 ^b	0.99±0.12
SS Cyg(A)	37±5	-	-3.29±0.01	1.59±0.01	-	-	11.74±0.13	36.75±0.27	13.72±0.09	-	1.19±0.02	0.704±0.002
SS Cyg(B)	37±5	-	5.72±0.05	1.61±0.03	-	-	11.58±0.06	-	17.28±0.40	-	1.19±0.02	0.704±0.002
V516 Cyg	-	1.78±0.16	-1.93±0.15	-	11.14±0.22	-	10.74±0.28	48.09±3.41	-	-	-	-
V542 Cyg	-	-4.45±0.53	-4.97±0.33	0.31±0.59	-	-	10.26±7.92	30.67±7.12	18.88±2.28	-	-	-
V792 Cyg	-	0.41±0.20	-2.28±0.18	0.86±0.10	11.45±0.56	31.99±3.52	11.78±0.74	32.25±3.07	31.64±10.14	-	-	-
V1504 Cyg	-	-4.24±0.19	-4.61±0.17	-	11.24±1.32	43.13±4.39	8.63±4.47	33.36±2.35	-	-	-	-
AB Dra	<55	-	1.45±0.21	-	-	-	15.73±4.23	52.74±15.46	-	-	-	-
EX Dra	85.8±0.6	21.55±0.39	14.92±0.38	19.47±0.40	20.35±0.43	-	18.17±0.55	-	31.49±1.03	-	0.78±0.02	0.59±0.02
AH Eri	-	-3.37±0.34	-4.85±0.30	-	10.86±0.94	35.83±4.03	6.54±0.79	38.51±2.84	-	-	-	-
IR Gem	-	-3.62±0.11	-3.97±0.09	-	7.75±0.21	34.53±1.08	7.83±0.71	24.27±0.60	-	-	-	-
U Gem	69.7±0.7	-1.11±0.04	-2.02±0.03	1.54±0.03	-	-	12.99±1.55	42.70±1.50	13.56±0.50	-	1.26±0.12	0.57±0.07
X Leo	-	3.33±1.75	-1.51±0.24	-	-	-	13.95±1.31	43.11±3.35	-	-	-	-
CY Lyr	-	-4.16±0.14	-4.76±0.20	0.25±0.16	-	-	14.17±2.98	35.03±2.12	-	-	-	-
V419 Lyr	-	-	-6.36±0.48	-0.48±0.37	-	-	-	36.41±6.77	-	-	-	-
BI Ori	-	2.10±0.27	0.07±0.24	0.77±0.16	-	-	15.5±1.36	32.96±8.65	14.26±3.24	-	-	-
CN Ori	67±3	-4.40±0.13	-4.44±0.40	0.26±0.05	-	-	12.23±2.41	40.45±5.35	-	-	0.74±0.10	0.49±0.08
V1159 Ori	-	-4.53±0.40	-5.39±0.40	-0.01±0.08	-	-	10.10±2.10	35.44±1.53	-	-	0.7-0.9 ^c	~0.11
HX Peg	-	2.16±0.21	0.10±0.21	2.79±0.55	13.36±0.97	51.97±11.80	11.38±1.06	44.45±17.10	16.66±1.04	-	-	-
IP Peg	68	13.91±0.13	15.25±0.16	27.44±0.16	19.41±0.23	-	18.54±0.21	-	20.18±0.13	-	1.15±0.10	0.67±0.08
RU Peg	33±5	-	-5.22±0.13	0.04±0.03	-	-	6.90±1.16	25.33±0.27	31.05±3.67	30.55±9.12	1.21±0.19	0.94±0.04
GK Per	68-73	6.59±0.06	5.33±0.10	14.54±0.10	9.33±0.11	-	10.45±0.18	-	12.13±0.08	-	0.87±0.24 ^d	0.48±0.32

Table 3. *Continued*

Target	i	EW ($H\beta$)	EW ($H\gamma$)	EW (HeII)	FWHM ($H\beta$)		FWHM ($H\gamma$)		FWHM (HeII)		$M_1(M_\odot)$	$M_2(M_\odot)$
					Emission	Absorption	Emission	Absorption	Emission	Absorption		
KT Per	-	-1.39±0.06	-2.28±0.05	1.06±0.04	-	-	15.15±0.66	44.50±1.59	21.92±1.35	-	-	-
TZ Per	-	-	-2.35±0.16	0.43±0.11	-	-	9.50±0.61	36.52±3.79	-	-	-	-
TY Psc	-	-7.40±0.05	-8.77±0.05	0.76±0.03	-	45.71±0.73	-	46.80±0.38	30.75±2.93	-	-	-
VZ Pyx	-	15.90±0.42	8.16±0.44	-	17.08±0.44	-	15.30±0.64	-	-	-	-	-
AW Sge	-	-	-3.19±0.25	0.01±0.13	-	-	-	66.59±8.48	-	-	-	-
RZ Sge	-	-0.03±0.25	-4.47±0.21	-	15.02±1.30	44.28±6.15	17.02±1.66	50.31±4.48	-	-	-	-
V893 Sco	-	35.74±2.76	25.27±3.14	3.71±0.33	34.95±2.91	-	31.59±3.20	-	58.22±8.19	-	0.5–0.6 ^e	~0.14
NY Ser	-	-	-7.63±0.67	-	-	-	-	62.23±44.42	-	-	-	-
DI UMa	-	-2.56±0.92	-2.48±0.76	-	-	-	-	17.50±6.65	-	-	-	-
ER UMa	-	-5.70±0.06	-6.94±0.05	0.90±0.03	11.97±0.37	42.98±0.90	11.64±0.53	41.21±0.45	27.20±2.10	-	-	-
IY UMa	86.8±1.5	8.93±0.05	16.64±0.07	13.31±0.05	22.36±0.16	-	33.45±1.11	-	32.04±0.32	-	0.86±0.11 ^f	0.12±0.02
SS UMi	-	50.76±1.61	35.45±1.19	5.31±0.96	30.32±0.95	-	28.08±5.95	-	-	-	-	-